Research Article

Kang He, Yu Chen*, and Mengjun Mei

Study on influencing factors of photocatalytic performance of CdS/TiO_2 nanocomposite concrete

https://doi.org/10.1515/ntrev-2020-0074
received June 01, 2020; accepted September 02, 2020

Abstract: In this study, a high-energy ball mill was used to composite nano-TiO_2 and CdS, and three kinds of nanocomposite photocatalysts TiO_2, CdS/TiO_2-R400, and CdS/TiO_2-R600 were prepared, which can respond to visible light. The photocatalytic concrete test block was prepared by mixing the nanocomposite photocatalyst and other masses with cement by incorporation method. To study the effect of the photocatalyst content on the photocatalytic performance of nanoconcrete, a total of four catalyst contents (0, 2%, 5%, and 8%) were set. The effects of high-temperature treatment (400°C) and different light sources (ultraviolet and visible light) on photocatalytic efficiency were also considered. The results show that the catalytic efficiency of CdS/TiO_2-R400 under two light sources is higher than that of the other two photocatalysts. Compared to ultraviolet light sources, the photocatalytic efficiency of CdS/TiO_2 nanocomposite concrete under visible light is lower, and the efficiency is below 9%. The optimal amounts of CdS/TiO_2 nanocomposite photocatalyst under ultraviolet and visible light are 2% and 5%, respectively. The high-temperature treatment can improve the photocatalytic performance of CdS/TiO_2 nanocomposite photocatalyst by 2% to 3%.

Keywords: photocatalytic concrete, nanocomposite, CdS/TiO_2, degradation rate, visible light

1 Introduction

Since the industrial revolution, fossil energy has become an indispensable energy source for human beings, but the environmental pollution problems caused by it have become more and more serious; on the other hand, with the increase in the number of cars, the emissions of automobile exhausts have become larger and larger. Among them, nitrogen oxides (NO_x) and SO_2 seriously affect the quality of urban air and threaten the health of urban residents. When academia discovered that water molecules on the surface of titanium dioxide electrode would decompose under ultraviolet light, this new material TiO_2 attracted much attention. With the deepening of research, the concept of using nanocomposite treat pollutants has been proposed and accepted by many people [1,2]. TiO_2 has the advantages of safety and non-toxicity, low price, high catalytic activity, and good stability. It is recognized as the best photocatalyst and has a good application prospect in the field of environmental pollution treatment. However, TiO_2 has a wide bandgap (anatase phase 3.2 eV), which can only be excited by ultraviolet light source, and the utilization rate of sunlight is only 3% to 5%, which greatly limits the application of TiO_2 under general conditions [3]. Therefore, by modifying TiO_2, expanding its response range to sunlight, and improving the utilization rate of sunlight has become a research hotspot. There are many studies on the modification of TiO_2 photocatalysts. In terms of semiconductor recombination, semiconductor materials with a more negative conduction band potential and smaller forbidden bandwidth than TiO_2, such as CdS, PbS, CdSe, and Cu_2O nanoparticles, are used for sensitization [4–8]. The semiconductor CdS has a bandgap of 2.42 eV and an excitation wavelength of 495 nm or less, which has a good absorption effect on sunlight. Through the synergistic effect of different forbidden bandwidths between semiconductors, the light stability of the catalyst is enhanced, and the

* **Corresponding author: Yu Chen,** College of Civil Engineering, Fuzhou University, Fuzhou, 350116, China,
e-mail: kinkingingin@163.com, tel: +86 18030219629
Kang He, Mengjun Mei: College of Civil Engineering, Fuzhou University, Fuzhou, 350116, China

recombination probability of photo-generated carriers is reduced, so that the photocatalytic performance of the material is effectively improved [9]. The role of TiO_2 phase composition, nanocrystalline sizes, carbon content in its different forms in establishing static and dynamic magnetic response of our samples will be discussed by Typek et al. [10]. Ruot et al. [11] used nano-TiO_2 cement paste and cement mortar to degrade rhodamine B. The results show that the type of cement has little effect on the photocatalytic performance. Shen et al. [12] covered the surface of the prepared concrete with tens of nanometers of C–S–H and TiO_2 nanoparticles. The results show that photocatalytic ultra-smooth concrete surfaces can effectively degrade methylene blue (MB). Teh et al. [13] discovered through research that higher specific surface area can promote the adsorption of more reactant molecules to the catalyst surface, thereby avoiding the recombination of photo-generated electron–hole pairs. The low grain size increases the specific surface area of the catalyst and promotes the photogenic support to turn to the surface of the catalyst to enhance the interaction with the reactant molecules [14]. Wang et al. [15] prepared a concrete pavement with emulsified asphalt as the carrier and nano-TiO_2 as a photocatalytic coating. The results showed that the nano-TiO_2 content in the coating was 8% and the spraying amount was 400 g/m^2. The sidewalk NO_x degradation rate was the highest. Two asphalt emulsions and one cement mortar are used in the right lane and emergency lane of highway sections. After comparison, it was found that the asphalt emulsion-based substrate still has a good NO degradation effect after 572 days [16]. Wang et al. [17–19] used photocatalytic degradation of phenol with anatase phase TiO_2 with different grain sizes to investigate the effect of grain size on the photocatalytic performance of anatase phase TiO_2. The results show that when the grain size is increased from 6.6 to 26.6 nm, the photocatalytic degradation rate of TiO_2 nanoparticles in the anatase phase increases significantly. They believe that the increase in grain size of the anatase phase TiO_2 can suppress the undesired hydroquinone–benzoquinone redox reaction, thereby promoting the complete decomposition of phenol and phenolic compounds. Saeli et al. [20–22] prepared a lime mortar containing 5 wt% Ag-TiO_2 and studied the removal activity of nitrous oxide (NO_x) and volatile organic compounds (VOC). The addition of dopants did not significantly change the physical properties or curing of the lime mortar but showed excellent photocatalytic activity in sunlight. Chen et al. [23,24] studied the effect of pH on the photocatalytic degradation of rhodamine B by TiO_2 using a spectrophotometric method. The results showed that the photocatalytic degradation rate of rhodamine B by TiO_2 was higher in acidic conditions than in alkaline conditions. Yang et al. [25] prepared silver and vanadium oxide co-doped TiO_2 by a one-step sol–gel solvothermal method in the presence of a triblock copolymer surfactant (P123). Song et al. [26] prepared Cu and N co-doped TiO_2 nanoparticles and studied the effects of different amounts of Cu and N doping on the photocatalytic activity of TiO_2. Shen et al. [27] prepared N and Ce co-doped TiO_2 by sol–gel method. The co-doped TiO_2 can photocatalytically degrade nitrobenzene under visible light.

Nanoconcrete as an effective combination of nanotechnology and traditional civil engineering has broadened the application range of nanotechnology and nanomaterials, and also solved many problems that traditional concrete materials are difficult to solve. This area has also produced a lot of research results in recent years [28–32]. Zhang et al. [33] evaluated the flexural strength and durability (carbonization resistance, penetration resistance, cracking resistance, freeze–thaw resistance) of nano-SiO_2 cement-based composite materials through experimental research. Tekin et al. [34,35] studied the effects of WO_3 and Bi_2O_3 additives on the micron and nanometer scales on the radiation shielding properties of hematite serpentine concrete (HSC). He et al. [36] replaced the traditional concrete in GFRP concrete composite columns with a new type of nanoconcrete and carried out a series of experimental studies on the mechanical properties of this new type of composite column. Cheng et al. [37–41] added a certain amount of nano-siO_2 to concrete to improve the durability of concrete. Al-Swaidani [42] studied the efficiency of adding concrete binder to volcanic slag on a nanometer scale. In recent years, a new method for producing heterogeneous photocatalysts, a high-energy ball milling method, has been proposed. The high-energy ball milling method is also called mechanochemical method. The substance undergoes chemical changes or physical and chemical changes due to the action of mechanical forces. The method can realize a reaction that can occur only under chemical or high-temperature conditions under normal temperature conditions. In this paper, a high-energy ball mill was used to combine TiO_2 and CdS through mechanochemical action to make a CdS/TiO_2 nanocomposite photocatalyst. Then, the nanocomposite CdS/TiO_2 was replaced by cement by an incorporation method, and the effects of different dosages (0, 2%, 5%, and 8%) on the photocatalytic performance of concrete were studied.

2 Testing process

2.1 Materials and instruments

The main instruments and consumables in this test include QM-QX2L omnidirectional planetary ball mill; UV-2600 ultraviolet visible spectrophotometer; TG16-WS high-speed centrifuge; CJJ78-1 magnetic stirrer; SX-4-10 medium temperature box resistance furnace; FA1004 analytical balance; small pure slurry mixer; 250 W high-pressure mercury lamp; 500 W long arc xenon lamp; 500 mL/1,000 mL beakers; 5 mL pipettes; pipette tips; 5 mL centrifuge tubes; 4 mL quartz cuvettes; PO42.5 Portland cement; 2 mm machine sand. The reagents used in the catalytic performance test are shown in Table 1.

2.2 Photocatalytic performance evaluation method

As there is currently no uniform photocatalytic performance evaluation method in the world, this paper uses the latest x method, the method used in this experiment was to use a Shimadzu UV-2600 UV-visible spectrophotometer to measure the absorbance (Abs) of the methyl orange solution at a peak of 464 nm. Then according to the initial and the absorbance of the solution at each time point A_0 and A_n, use formula (1) to analyze the degradation of methyl orange. The degradation rate of methyl orange is used to represent the catalytic performance of photocatalytic concrete, and the catalytic performance of composite catalysts is evaluated.

$$\text{Degradation rate} = \frac{A_0 - A_n}{A_0} \tag{1}$$

In formula (1), A_0 is the initial absorbance of methyl orange when photocatalytic concrete is added and the equilibrium of adsorption and desorption is reached. A_n is the absorbance of methyl orange solution at each time point after light.

2.3 Preparation of composite catalyst

First, weigh 2 g CdS powder and 18 g TiO_2 powder into a 500 mL corundum ball mill pot with a mass ratio of 1:9. The material of the ball in the tank is zirconium dioxide. The planetary ball mill is used for ball milling at a speed of 400 rpm for 2 h, as shown in Figure 1, and the powder was then weighed and ground with a rotating ball at a speed of 600 rpm for 2 h.

CdS and TiO_2 powder were added to a 500 mL corundum ball mill at a mass ratio of 1:9 for ball milling treatment, as shown in Figure 1. The ball milling rates are 400 rpm and 600 rpm, corresponding to two different CdS/TiO_2 nanocomposite photocatalyst CdS/TiO_2-R400 and CdS/TiO_2-R600, respectively. The ball-milling treatment time for both nanocomposite photocatalyst was 2 h.

Due to the heat generated during the ball milling process, the tank body became hot. Therefore, the ball milling tank could not be taken out immediately after the ball milling was finished. After the ball milling tank was cooled to room temperature, it could be removed to avoid burns. After taking out the ball mill tank, an appropriate amount of absolute ethanol was added to the tank, and the powder of the composite material was diffused into the absolute alcohol with sufficient agitation. Finally, the processed composite material powder was poured into a stainless steel tray and dried in a drying box. The solid material was collected and ground into a mortar. One part was directly put into the labeling record in the sample bottle, and the other part was put into the calcining kettle and put into the muffle furnace for calcination at 400°C for 4 h. After being calcined and cooled for 12 h, it was taken out into the sample bottle and labeled with the record.

2.4 Preparation of photocatalytic concrete

In this experiment, the photocatalytic concrete was made by the internal mixing method. Materials used in making concrete: PO42.5 Portland cement, ordinary fine

Table 1: Main reagents

Name	Molecular formula	Quality of raw materials	Place of origin
Anatase titanium dioxide	TiO_2	Analytical pure	Shanghai, China
Cadmium sulfide	CdS	Analytical pure	Shanghai, China
Methyl orange	$C_{14}H_{14}N_3NaO_3S$	Analytical pure	Shanghai, China
Absolute ethanol	C_2H_5OH	99.5%	Tianjin, China

(a) (b)

Figure 1: Preparation of nanocomposite catalyst. (a) Ball mill (b) preparing process.

sand with a particle size greater than 2 mm, water. The mixing ratio of cement:water:sand was 1:0.4:1. Each concrete test block has a diameter of 80 mm and a thickness of 10 mm. The average mass is 100 g. A total of three nanocatalysts were prepared in this experiment, as shown in Table 2. To study the effect of high temperature on the photocatalytic efficiency of the catalyst, each type of nanocatalyst has two temperature treatment methods, one is room temperature and the other is 400°C. The photocatalytic concrete test blocks were prepared by replacing the catalyst with cement based on the principles of 0%, 2%, 5%, and 8% mass, respectively. Figure 2 shows all the nanocatalysts and their corresponding photocatalytic nanoconcrete samples in the experiment. After the test block was manufactured, it was placed in a standard curing room for 7 days. After the curing was completed, the photocatalytic performance of the test block could be tested.

2.5 Photocatalytic performance test

About 300 mL of 10 mg/L methyl orange solution was poured into the beaker, and then the cured photocatalytic concrete test block was put into the methyl orange solution. Finally, the beaker was moved to a photocatalytic reaction box and stirred with a magnetic stirrer for 30 min before the photocatalytic treatment. When the solution reached the equilibrium of adsorption and desorption, 4 mL of supernatant was removed and placed in a centrifuge tube. At the same time, as shown in Figure 3(a), when the ultraviolet light source in the box was turned on, 4 mL of supernatant was extracted every 30 min. The total duration of light in each experiment was 2 h. The other group used the same materials and steps and was irradiated with fluorescent light for 2 h, as shown in Figure 3(b). Then, when the solution was centrifuged, the supernatant was collected. Spectrophotometer measurement was used to measure the absorbance of the solution at different exposure times. According to the absorbance A corresponding to different photocatalytic time, the degradation rate of methyl orange was obtained, and the photocatalytic performance of the nanocomposite catalyst was evaluated.

Table 2: Nanocomposite catalyst

Name	Ingredient	Working speed of ball mill (rpm)	Mass ratio (CdS/TiO_2)
TiO_2	TiO_2	—	—
CdS/TiO_2-R400	CdS and TiO_2	400 rpm	1:9
CdS/TiO_2-R600	CdS and TiO_2	600 rpm	1:9

3 Test results and analyses

3.1 Photocatalytic performance of nanoconcrete

A set of plain concrete control group was set up in the experiment. The photocatalytic performance of the plain concrete test block under ultraviolet light and fluorescent light was tested to obtain the methyl orange self-degradation rate in the presence of the plain concrete.

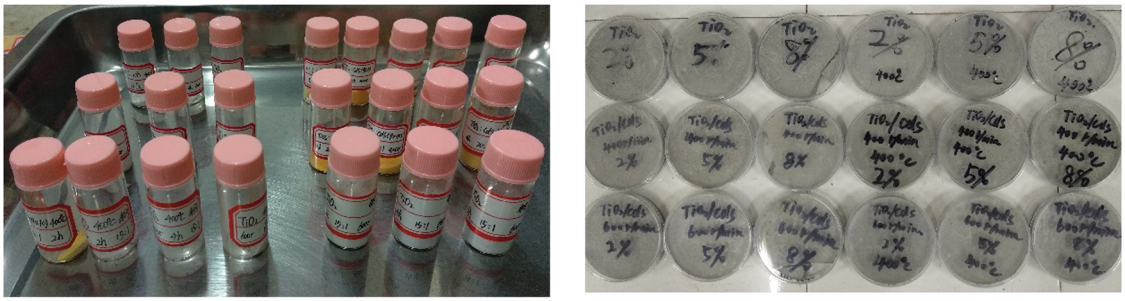

(a) (b)

Figure 2: Nanocatalysts and photocatalytic nanoconcrete samples. (a) Nanocatalyst sample. (b) Photocatalytic nanoconcrete samples.

Then it was compared with three kinds of photocatalytic concrete under ultraviolet light and visible light to decompose methyl orange.

As shown in Figure 4(a), under ultraviolet light irradiation, the degradation rate of methyl orange in the plain concrete test block group gradually increased with the increase in the light time. In the 2% photocatalytic concrete group, with the increase of light time, the degradation rate of methyl orange gradually increased, and the increasing trend was more obvious. As shown in Figure 4(b), under visible light irradiation, the degradation rate of methyl orange was almost zero in the first 30 min of the plain concrete test block group, and the degradation rate (absolute value) gradually increased with the increase in the light time. In the 2% photocatalytic concrete group, the degradation rate slowly increased in the first 60 min, and the degradation rate began to decrease with time.

Comparing Figure 4(a) and (b), it is found that the large difference in degradation rate between the two groups is partially due to the difference between the two light source lamps. In this test, the ultraviolet light source is a mercury lamp, which generates less heat during work and has less impact on the experiment; while the visible light source is a xenon lamp, which generates a large amount of heat during work, which raises the temperature of the methyl orange solution. When the solution was exposed to light for 2 hours, the temperature of the solution system reached 60°C, and the solubility of methyl orange reached the maximum at about 55°C. Therefore, when the temperature of the solution is increased due to the xenon lamp irradiation, the undissolved methyl orange fine particles in the original solution diffuse into the solution, the color of the solution deepens, and the absorbance increases. Therefore, in visible light, the degradation rate of methyl orange in the plain concrete group is negative and the absolute value is increasing.

(a) (b)

Figure 3: Photocatalytic reaction box. (a) UV light source. (b) Visible light source.

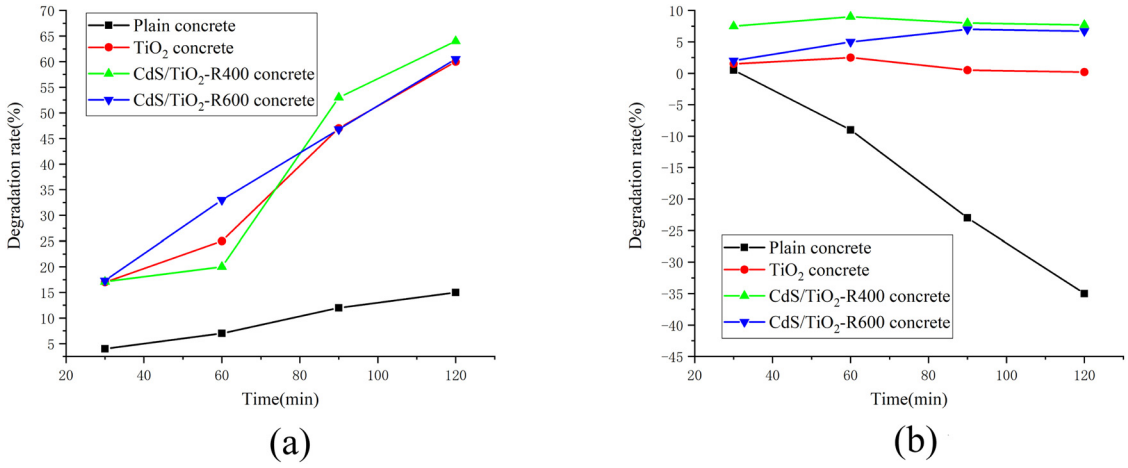

Figure 4: Comparison of photocatalytic performance between plain concrete and nanocomposite concrete. (a) Ultraviolet light (b) visible light.

3.2 Effect of catalyst types on photocatalytic performance of nanoconcrete

The photocatalytic performance of photocatalytic concrete is related to the type of catalyst incorporated. This test evaluated the catalytic performance of three different photocatalytic concretes, TiO_2 concrete, CdS/TiO_2-R400 concrete, and CdS/TiO_2-R600 concrete. It needs to be explained here that the degradation rate of the ordinate in Figure 5 is the degradation rate of the methyl orange test solution obtained by the photocatalytic reaction of each group of samples after 2 h. In Figure 5, the black, red, and blue columns correspond to nanocomposite photocatalytic concrete added with three different catalysts TiO_2, CdS/TiO_2-R400, and CdS/TiO_2-R600, respectively. To further study the difference between the photocatalytic performance of three different catalysts under ultraviolet and visible light sources, two sets of tests were set up, as shown in Figure 5(a) and (b), and each group covered 2%, 5%, and 8% catalyst contents. As shown in Figure 5(a), under the action of ultraviolet light source, when the catalyst content is the same, the photocatalytic performance of CdS/TiO_2-R400 in the three nanocomposite photocatalytic concrete is slightly higher than the other two catalysts, but the gap between the three catalysts is within 2%. Therefore, under the action of the ultraviolet light source, the difference between the three different catalysts is not obvious, and the catalytic efficiency of the three nanocomposite photocatalytic concretes is between 50% and 65%.

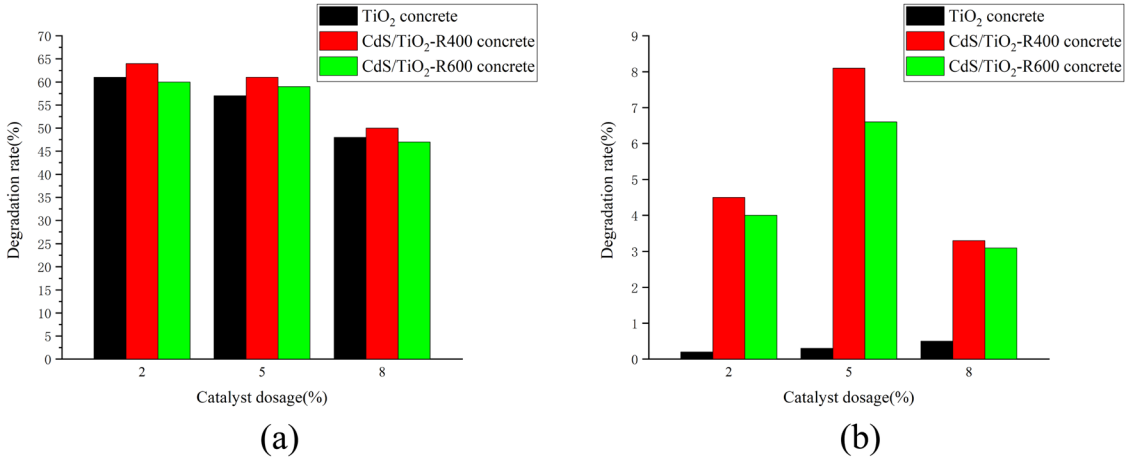

Figure 5: Photocatalytic efficiency of photocatalytic concrete with different catalyst types. (a) Ultraviolet light (b) visible light.

As shown in Figure 5(b), CdS/TiO_2-R400 concrete has the best catalytic effect under visible light irradiation, followed by CdS/TiO_2-R600 concrete, and the worst effect is pure TiO_2 concrete. Theoretically, pure TiO_2 concrete has very low catalytic activity under visible light. Because no filter was set during the visible light irradiation in this experiment, TiO_2 absorbed part of the ultraviolet light in the xenon light source, so that pure TiO_2 concrete showed catalytic activity under visible light.

3.3 Effect of catalyst content on the catalytic performance of nanoconcrete

For the same nanocomposite photocatalytic concrete, when the amount of the catalyst is changed, its photocatalytic performance will fluctuate. For this reason, this experiment designed a total of 2%, 5%, and 8% of three catalyst levels. Similarly, Figure 6(a) represents the degradation rate of nanocomposite photocatalytic concrete under ultraviolet light source, and Figure 6(b) represents the degradation rate under visible light source.

As shown in Figure 6(a), when the catalyst types are the same, under ultraviolet light irradiation, the degradation rate of methyl orange gradually decreases as the amount of the catalyst increases. When the catalyst content is 2%, the photocatalytic concrete has the best catalytic performance, and the law is the same for the three different types of catalysts.

Under visible light irradiation, in Figure 6(b), with the increase of the dosage, the degradation rate of methyl orange increases first and then decreases, and there is an optimal dosage of 5%. Compared with the photocatalytic efficiency of three nanocomposite catalysts under the action of ultraviolet light source, the amount of catalyst in the visible light source has a significant effect on the photocatalytic performance of nanoconcrete. This law is especially evident in CdS/TiO_2-R400 concrete and CdS/TiO_2-R600 concrete. When the catalyst content is 5%, their photocatalytic efficiency is almost doubled when the content is 2% and 8%. However, nanocomposite photocatalytic concrete has low photocatalytic efficiency under visible light, and all catalytic efficiency is below 9%.

3.4 Effect of high temperature on catalyst performance

Because the composite CdS/TiO_2 catalyst is collided by the balls at high speed in the ball mill tank, the crystal structure will have defects. The high-temperature calcination can reduce the defects of the crystal structure and reduce the impurities. However, the effect of high-temperature treatment on the performance of composite CdS/TiO_2 catalysts needs to be clarified. In this test, a part of the composite catalyst was first placed in a muffle furnace and calcined at a high temperature of 400°C for 2 hours, and then the calcined composite catalyst was used to make photocatalytic concrete. The manufacturing method was the same as that of the catalyst without the high temperature treated concrete. After curing, test its photocatalytic performance, compare the

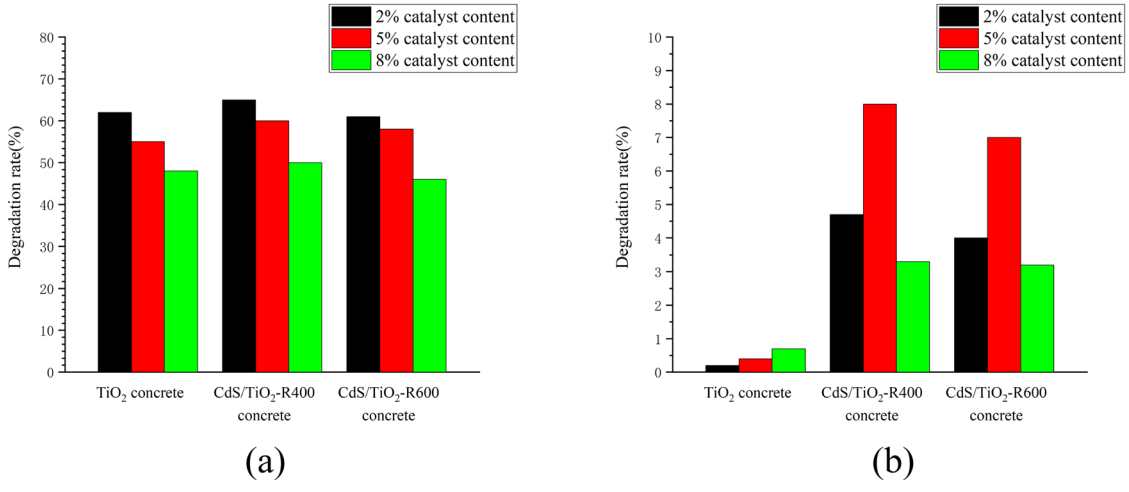

Figure 6: Photocatalytic efficiency of photocatalytic concrete with different catalyst contents. (a) Ultraviolet light, (b) visible light.

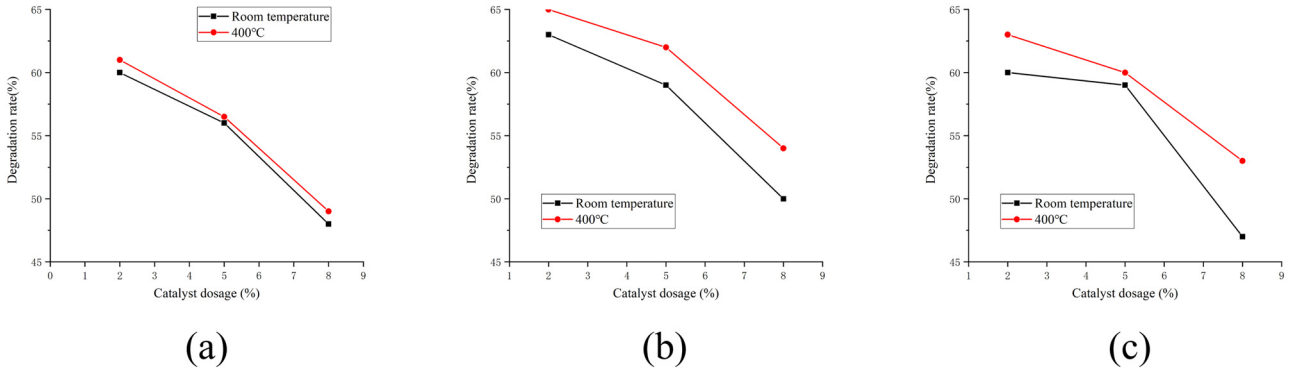

Figure 7: Comparison of photocatalytic performance of catalysts treated at different temperatures under ultraviolet light sources. (a) TiO_2 concrete, (b) CdS/TiO_2-R400 concrete, (c) CdS/TiO_2-R600 concrete.

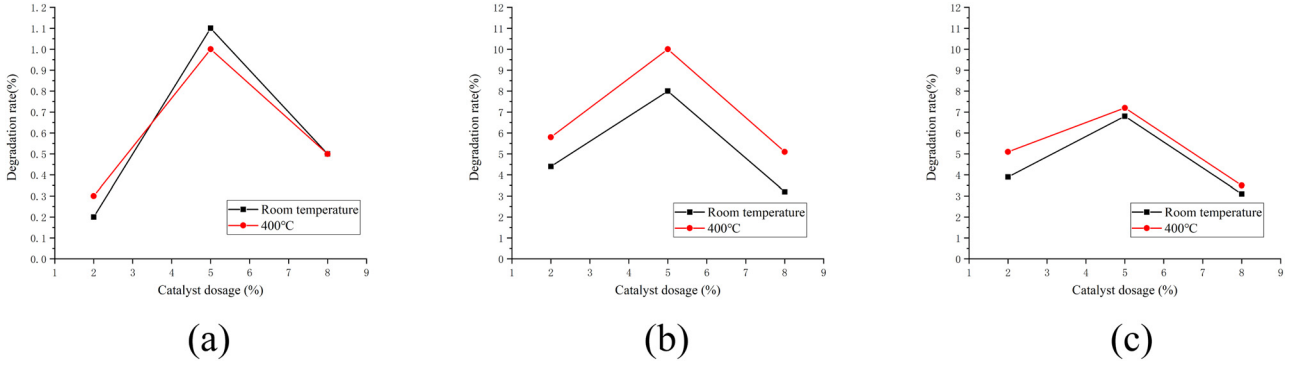

Figure 8: Comparison of photocatalytic performance of catalysts treated at different temperatures under visible light sources. (a) TiO_2 concrete, (b) CdS/TiO_2-R400 concrete, (c) CdS/TiO_2-R600 concrete.

catalytic performance of the concrete test block made of the composite catalyst calcined at high temperature with the concrete test block made of the untreated composite catalyst, and explore the effect of high temperature on the performance of the composite photocatalyst.

Under the action of ultraviolet light source, the red lines representing the degradation rate of the nanocomposite photocatalytic concrete after the catalyst is treated at 400°C in Figure 7 are above the catalyst at normal temperature. Therefore, the high-temperature treatment at 400°C promoted the photocatalytic performance of the three nanocatalysts. As shown in Figure 7(a) and (b), for catalysts TiO_2 and CdS/TiO_2-R400, the increase in photocatalytic efficiency after 400°C high-temperature treatment does not change with the increase in the dosage of catalyst. As shown in Figure 7(a) and (b), the two lines are approximately parallel. However, as shown in Figure 7(c), for catalyst CdS/TiO_2-R600, the effect of 400 high-temperature treatment on the improvement of photocatalytic efficiency is significantly less than the dosage of 2% and 8% when the catalyst content is 5%.

As shown in Figure 8, under the action of visible light, the catalytic efficiency of CdS/TiO_2-R400 and CdS/TiO_2-R600 catalysts was slightly improved after 400°C high-temperature treatment. The photocatalytic efficiency of the TiO_2 catalyst after 400°C high-temperature treatment decreased when the content was 5%. However, the catalytic efficiency of the TiO_2 catalyst under visible light is less than 1.2%, so this discrete fluctuation cannot be considered and does not affect the evaluation of the effect of high temperature on the nanocatalyst.

4 Conclusions

The differences in photocatalytic efficiency of three different nanocomposite catalysts, TiO_2, CdS/TiO_2-R400, and CdS/TiO_2-R600, are more pronounced under the action of visible light than under the action of ultraviolet light. However, the catalytic efficiency of CdS/

TiO_2-R400 under the two light sources is higher than the catalytic efficiency of the other two photocatalysts.

Under the action of ultraviolet rays, the catalytic efficiency of the three kinds of nanocomposite photocatalytic concrete is between 50% and 65%. Compared with ultraviolet light sources, the photocatalytic efficiency of CdS/TiO_2 nanocomposite photocatalytic concrete under visible light is lower, and the catalytic efficiency is less than 9%.

The amount of nanocomposite catalyst in photocatalytic concrete has a significant effect on its photocatalytic performance, and the optimal amount of CdS/TiO_2 nanocomposite catalyst under visible light source and ultraviolet light source is different. Under the action of ultraviolet light, when the catalyst content is 2%, the catalytic performance of photocatalytic concrete is the best. Under visible light, when the catalyst content is 5%, its photocatalytic efficiency is almost twice as high as when the catalyst content is 2% and 8%.

After the CdS/TiO_2 nanocomposite catalyst was calcined at 400°C, the photocatalytic performance was slightly improved under the ultraviolet and visible light sources. The increase in the photocatalytic efficiency is basically between 2% and 3%.

Acknowledgments: This research work was supported by the National Natural Science Foundation of China (No. 51778066 and 52078138).

Conflict of interest: The authors declare no conflict of interest regarding the publication of this paper.

References

[1] Fujishima A, Honda K. Electrochemical photolysis of water at a semiconductor electrode. Nature 1972;238(5358):37–8.
[2] Yi ZG, Tang Q, Jiang T, Cheng Y. Adsorption performance of hydrophobic/hydrophilic silica aerogel for low concentration organic pollutant in aqueous solution. Nanotechnol Rev. 2019;8(1):266–74.
[3] Kumar SG, Devi LG. Review on modified TiO_2 photocatalysis under UV/visible light: Selected results and related mechanisms on interfacial charge carrier transfer dynamics. J Phys Chem A. 2011;115(46):13211–41.
[4] Soon HK, Lee W, Kim HS. Effects of CdS sensitization on single crystalline TiO_2 nanorods in photoelectrochemical cells. Mater Lett. 2012;85:74–6.
[5] Zeng T, Tao HZ, Sui XT, Zhou XD, Zhao XJ. Growth of free-standing TiO_2 nanorod arrays and its application in CdS quantum dots-sensitized solar cells. Chem Phys Lett. 2011;508;130–3.
[6] Im S, Kim H, Kim S, Kim S, Seok S. All solid state multiply layered PbS colloidal quantum-dot-sensitized photovoltaic cells. Energy Env Sci. 2011;4:4181–6.
[7] Lina JD, Shen Q, Sato A, Katayama K, Sawada T, Toyoda T. Optical absorption and ultrafast carrier dynamics characterization of CdSe quantum dots deposited on different morphologies of nanostructured TiO_2 films. Energy Env Sci. 2007;27:1514–20.
[8] Xue J, Shen Q, Liang W, Liu X, Xu B. Controlled synthesis of coaxial core-shell TiO_2/Cu_2O heterostructures by electrochemical method and their photoelectrochemical properties. Mater Lett. 2013;92:239–42.
[9] Xie Y, Ali G, Yoo SH, Cho SO. Sonication-assisted synthesis of CdS quantum-dot-sensitized TiO_2 nanotube arrays with enhanced photoelectrochemical and photocatalytic activity. ACS Appl Mater Interfaces. 2010;2:2910–4.
[10] Typek J, Guskos N, Zolnierkiewicz G, Pilarska M, Guskos A, Kusiak-Nejman E, et al. Magnetic properties of TiO_2/graphitic carbon nanocomposites. Rev Adv Mater Sci. 2019;58(1):107–22.
[11] Ruot B, Plassais A, Olive F, Guillot L, Bonafous L. TiO_2-containing cement pastes and mortars: Measurements of the photocatalytic efficiency using rhodamine B-based colorimetric test. Sol Energy. 2009;83:1794–801
[12] Shen W, Zhang C, Li Q, Zhang W, Cao L, Ye J. Preparation of titanium dioxide nano particle modified photocatalytic self-cleaning concrete.
J Clean Prod. 2015;87:762-5.
[13] Teh CM, Mohamed AR. Roles of titanium dioxide and ion-doped titanium dioxide on photocatalytic degradation of organic pollutants (phenolic compounds and dyes) in aqueous solutions: A review. J Alloy Compd. 2011;509(5):1648–60.
[14] Shi J, Zheng J, Wu P. Preparation, characterization and photocatalytic activities of holmium-doped titanium dioxide nanoparticles. J Hazard Mater. 2009;161(1):416–22.
[15] Wang H, Jin K, Dong X, Zhan S, Liu C. Preparation technique and properties of nano-TiO_2 photocatalytic coatings for asphalt pavement. Appl Sci-Basel. 2018;8(11):2049.
[16] Bocci E, Riderelli L, Fava G, Bocci M. Durability of NO oxidation effectiveness of pavement surfaces treated with photocatalytic titanium dioxide. Arab. J Sci Eng. 2016;41(12):4827–33.
[17] Wang X, So L, Su R, Wendt S, Hald P, Mamakhel A, et al. The influence of crystallite size and crystallinity of anatase nanoparticles on the photo-degradation of phenol. J Catal. 2014;310:100–8.
[18] Xiao N, Li Z, Liu J, Gao Y. Effects of calcination temperature on the morphology, structure and photocatalytic activity of titanate nanotube thin films. Thin Solid Films. 2010;519:541–8.
[19] Smith YR, Kar A, Subramanian V. Investigation of physicochemical parameters that influence photocatalytic degradation of methyl orange over TiO_2 nanotubes. Ind Eng Chem Res. 2009;48:10268–76.
[20] Saeli M, Tobaldi DM, Rozman N, Skapin AS, Labrincha JA, Pullar RC. Photocatalytic nano-composite architectural lime mortar for degradation of urban pollutants under solar and visible (interior) light. Constr Build Mater. 2017;152:206–13.
[21] Boonen E, Akylas V, Barmpas F, Bottalico L, Boreave A, Cazaunau M, et al. Construction of a photocatalytic

de-polluting field site in the Leopold II tunnel in Brussels. J Env Manage. 2015;155:136–44.
[22] Maier W, Nilsson C, Holzer M, Lind J, Rosebom K. Photocatalytic plaster for indoor air purification, 1st national congress of construction mortars. Lisbon; 2005.
[23] Chen J, Ollis DF, Rulkens WH, Bruning H. Photocatalyzed oxidation of alcohols and organochlorides in the presence of native TiO_2 and metallized TiO_2 suspensions. Part (I): Photocatalytic activity and pH influence. Water Res. 1999;33(3):661–8.
[24] Cui Q, Feng B, Chen W, Wang JX, Lu X, Weng J. Effects of morphology of anatase TiO_2 nanotube films on photo-catalytic activity. J Inorg Mater. 2010;25(9):916–20.
[25] Yang X, Ma F, Li K, Guo Y, Hu J, Li W, et al. Mixed phase titania nanocomposite codoped with metallic silver and vanadium oxide: New efficient photocatalyst for dye degradation. J Hazard Mater. 2010;175(1–3):429–38.
[26] Song K, Zhou J, Bao J, Feng Y. Photocatalytic activity of (copper, nitrogen)-codoped titanium dioxide nanoparticles. J Am Ceram Soc. 2008;91(4):1369–71.
[27] Shen XZ, Liu ZC, Xie SM, Guo J. Degradation of nitrobenzene using titania photocatalyst co-doped with nitrogen and cerium under visible light illumination. J Hazard Mater. 2009;162(2–3):1193–8.
[28] Sanchez F, Sobolev K. Nanotechnology in concrete – A review. Constr Build Mater. 2010;24(11):2060–71.
[29] Reiterman P, Holcapek O, Zobal O, Keppert M. Freeze–thaw resistance of cement screed with various supplementary cementitious materials. Rev Adv Mater Sci. 2019;58(1):66–74.
[30] He K, Chen Y. Experimental evaluation of built-in channel steel concrete-filled GFRP tubular stub columns under axial compression. Compos Struct. 2019;219:51–68.
[31] He K, Chen Y, Yan Y. Axial mechanical properties of concrete-filled GFRP tubular hollow composite columns. Compos Struct. 2020;243:112174.
[32] Zhuang CL, Chen Y. The effect of nano-SiO_2 on concrete properties: A review. Nanotechnol Rev. 2019;8(1):562–72.
[33] Zhang P, Ling YF, Wang J, Shi Y. Bending resistance of PVA fiber reinforced cementitious composites containing nano-SiO_2. Nanotechnol Rev. 2019;8(1):690–8.
[34] Tekin HO, Sayyed MI, Issa SAM. Gamma radiation shielding properties of the hematite-serpentine concrete blended with WO_3 and Bi_2O_3 micro and nano particles using MCNPX code. Radiat Phys Chem. 2018;150:95–100.
[35] Tekin HO, Singh VP, Manici T. Effects of micro-sized and nano-sized WO3 on mass attenauation coefficients of concrete by using MCNPX code. Appl Radiat Isot. 2017;121:122–5.
[36] He K, Chen Y, Xie WT. Test on axial compression performance of nano-silica concrete-filled angle steel reinforced GFRP tubular column. Nanotechnol Rev. 2019;8(1):523–38.
[37] Cheng YK, Shi ZW. Experimental study on nano-SiO_2 Improving concrete durability of bridge deck pavement in cold regions. Adv Civ Eng. 2019;2019:5284913.
[38] Zhang P, Li QF, Chen YZ, Shi Y, Ling YF. Durability of steel fiber-reinforced concrete containing SiO_2 nano-particles. Materials 2019;12(13):2184.
[39] Zhang MH, Zhang WY, Xie FT. Experimental study on ASR performance of concrete with nano-particles. J Asian Archit Build Eng. 2019;18(1):3–9.
[40] Ye MY, Pan JH, Guo Z, Liu XY, Chen Y. Effect of ball milling process on the photocatalytic performance of CdS/TiO_2 composite. Nanotechnol Rev. 2020;9(1):558–67.
[41] Zhang MH, Zhang WY, Sun YY. Durability of concrete with nano-particles under combined action of carbonation and alkali silica reaction. J Asian Archit Build Eng. 2019;18(5):421–9.
[42] Al-Swaidani AM. Efficiency of nano-volcanic scoria in the concrete binder. SN Appl Sci. 2019;1(9):UNSP 980.